Atmos. Chem. Phys. Discuss., 7, 9283–9317, 2007
www.atmos-chem-phys-discuss.net/7/9283/2007/

Atmospheric Chemistry and Physics Discussions

Optical and geometrical characteristics of cirrus clouds over a mid-latitude lidar station

E. Giannakaki[1], **D. S. Balis**[1], **V. Amiridis**[2], **and S. Kazadzis**[1]

[1]Laboratory of Atmospheric Physics, Thessaloniki, Greece
[2]Institute for Space Applications and Remote Sensing, Athens, Greece

Received: 4 May 2007 – Accepted: 26 June 2007 – Published: 2 July 2007

Correspondence to: E. Giannakaki (egian@auth.gr)

Abstract

Optical and geometrical characteristics of cirrus clouds over Thessaloniki, Greece (40.6°, 22.9°) have been determined from the analysis of lidar and radiosonde measurements performed during the period from 2000 to 2006. Cirrus clouds are generally observed in a mid altitude region ranging from 7 to 12 km, with mid-cloud temperatures in the range from –65° to –25°C. A seasonality of cirrus geometrical and temperature properties is found. The cloud thickness ranges from 0.85 to 5 km and 37% of our cases have thickness between 2 and 3 km. The retrieval of cloud's optical depth and lidar ratio is performed using three different methods, taking into account multiple scattering effects. The mean optical depth is found to be 0.3±0.24 and the corresponding mean lidar ratio is 28±17 sr. Sub-visual, thin and opaque cirrus clouds are observed at 7.5%, 51% and 42.5% of the measured cases respectively. The multiple scattering errors of the measured effective extinction coefficients range from 20% to 60% depending on cloud optical depth. A comparison of the results between the three methods shows good agreement. In addition we present the advantages and limitations of each method applied. The temperature and thickness dependencies on optical properties have also been studied in detail. A maximum mid-cloud depth of ~3 km is found at temperatures around ~–45°C while there is an indication that optical depth increases with increasing thickness and mid-cloud temperature. No clear dependence of the lidar ratio values on the cloud temperature and thickness was found.

1 Introduction

Cirrus clouds are optically thin and non-black high, cold clouds composed by ice crystals (e.g. Eleftheratos et al., 2007). These clouds affect the Earth's climate through two opposite effects; an infrared greenhouse effect and a solar albedo effect. The contribution of each effect depends strongly on cirrus optical properties (e.g. Zerefos et al., 2003). Thin cirrus clouds usually cause a positive radiative forcing at the top of the

ACPD
7, 9283–9317, 2007

atmosphere, while thick cirrus clouds may produce cooling (Stephens and Webster, 1981; Fu and Liou, 1993; Fahey and Schumann, 1999). Generally, if the climate gets warmer some ice clouds will be replaced by longer-lasting water clouds. This fact will not only increase the cloud amount, but will change the balance between solar reflection and infrared emission (Platt et al., 1994). As cirrus clouds play a significant role in the radiative balance of the Earth's atmospheric system, a clear understanding of their properties at different geographical locations is highly essential for climate modeling studies.

The lidar technique is a very powerful tool to characterize the time and spatial evolution of the atmospheric aerosols, as well as to investigate the chemical and physical properties of cloud composing particles (Wang et al., 2005). Backscatter and Raman lidars have been used to retrieve information on geometrical and optical properties of clouds and aerosols layers through the application of different methods (e.g. Barrett and Ben-Dov, 1967; Viezee et al., 1969; Davis, 1969; Fernald et al., 1972; Platt, 1973; Platt, 1979; Klett, 1981; Fernald, 1984; Ansmann et al., 1992). Some physical parameters of primary concern are the extinction and backscatter coefficients as well as the cloud mean altitude and mid-cloud temperature, which play an important role in determining cloud radiative properties (Sunilkumar and Parameswaran, 2005).

Comstock and Ackerman (2002) have studied the optical and geometrical properties of tropical cirrus clouds and found that high clouds occur on average 44% of the time. Cadet et al. (2003) have presented climatology for sub-tropical cirrus clouds and showed that cirrus clouds are present more frequently at austral summer than the austral winter. The same study showed that 65% of the total cirrus observations are characterized as sub-visual, with an optical thickness of less than 0.03. The threshold of 0.03 for optical thickness measured at the wavelength of 694 nm was first proposed by Sassen and Cho (1992) in order to separate cirrus clouds to visible cirrus and sub-visual cirrus clouds. Goldfarb et al. (2001) found that sub-visual cirrus clouds constitute ~20% of total cirrus cloud occurrences for a mid-latitude lidar station in France. A mid-latitude cirrus climatology was also presented from Sassen and Campbell (2001)

ACPD
7, 9283–9317, 2007

showing that optical depth of cirrus clouds is greater than 0.3 for ~50% of detected cases. Seifert et al. (2007)[1] have studied optical properties of tropical cirrus clouds and found 13%, 50% and 37% for subvisual, thin and opaque cirrus clouds respectively. Many other studies have been performed and mainly focused on tropical cirrus clouds because of the high frequency of occurrence of sub-visual cirrus clouds and their significant influence on the Earth's atmospheric system (Comstock and Ackerman, 2002), as observed by SAGE (Stratospheric Aerosol and Gas Experiment) II (Wang et al., 1996; Wang et al. 1998). However, global cirrus statistics, and thus mid-latitude cirrus clouds climatological results, are essential for accurate climate simulations (Goldfarb et al., 2001).

The optical extinction of clouds is a key parameter in radiative transfer studies and therefore considerable effort has been put in its retrieval. Several methods to evaluate the optical depth of cirrus clouds using lidar measurements have been developed and applied in the past. Most of these methods depend on the solution of the standard lidar equation (Barrett and Ben-Dov, 1967; Viezee et al., 1969; Davis, 1969; Fernald et al. 1972; Platt, 1973; Platt, 1979; Klett, 1981; Fernald, 1984; Ansmann et al., 1992; Wandinger, 1998). A different technique to determine the optical depth of cirrus clouds from elastic lidar signal has also been developed which is based on the comparison of the backscattering signals just bellow and above the cloud assuming the lidar signals correctly represented the scattering medium (Platt, 1973; Young, 1995; Chen et al., 2002). However, these methods have never been compared or validated against each other using long term monitoring lidar measurements.

In this study, after a brief description of the lidar system used, we present a short description of the data analysis methods, along with a typical analysis case study. The main objective of this part of the study is to evaluate the benefits of applying various methodologies to the lidar measurements as well as to investigate the limits of their

[1]Seifert, P., Ansmann, A., Muller, D., Wandinger, U., and Althausen D.: Cirrus observations with Lidar, Radiosonde, and Satellite over the Tropical Indian Ocean During Northeast and Southwest Monsoon Seasons, J. Geophys. Res., in review, 2007.

applicability. Finally, climatology of mid-latitude cirrus clouds created from the analysis of lidar data collected in Thessaloniki over the period 2000–2006 is presented and discussed.

2 Instrumentation and data

A two wavelength combined Raman elastic-backscatter lidar located at the Laboratory of Atmospheric Physics (LAP), Thessaloniki, Greece (40.6°, 22.9°) is used to perform continuous measurements of suspended aerosol particles and cirrus clouds. The system is based on the second and third harmonic frequency of a compact, pulsed Nd:YAG laser, which emits pulses of 300 and 120 mJ output energy at 532 and 355 nm, respectively, with a 10 Hz repetition rate. The optical receiver is a 500 mm diameter telescope (1 mrad field of view). Three Hamamatsu 5600P-06 photomultipliers are used to detect the lidar signals at 532, 355 and 387 nm. The acquisition system is based on a three-channel LICEL Transient Digitizer working in both the analogue (12bits, 40 MHz) and the photon counting (8192 time bins 250 MHz) modes. The LAP lidar was successfully intercompared with the other European Aerosol Research Lidar Network (EARLINET) lidars, showing on the average an agreement of better than 5% for heights above 2 km in the backscatter coefficient (Matthias et al., 2004). More technical and measurement details concerning the system can be found at Balis et al. (2003) and Amiridis et al. (2005).

Within the EARLINET project, coordinated lidar measurements are being performed at 22 lidar stations located at 12 European countries. The measurements began in May 2000 and three synchronous observations per week were performed from May 2000 to November 2002. Most of the EARLINET stations continued this schedule also after 2002. In this study, we present lidar measurements at Thessaloniki, for cases when cirrus clouds were observed during the measurements for the entire period 2000–2006. Fifteen cases of Raman (night) measurements and fifty cases of daily measurements were found during the routine schedule of the measurements. For these measurements

ACPD
7, 9283–9317, 2007

EGU

temperature vertical profile data from radiosondes were used to yield the temperature of the base and top of cirrus cloud.

3 Methodology

In order to get reliable and quantitative results for the optical properties of cirrus clouds three different methods are briefly presented and used in this study. One main aspect of all methods is the accurate determination of cirrus cloud boundaries. This aspect is of major importance not only for the correct application of those methods, but also to obtain precise geometrical properties of cirrus clouds. The heights of the cirrus cloud base and top, obtained from the time averaged signals, are the first data quantities to be derived. The time averaged signals are first of all corrected for altitude range and background noise and consecutively the corrected signal profile is smoothed through a sliding average smoothing routine. The cloud-base altitude is defined as that altitude at which there is an increase in the system's signal level that equals two times the standard deviation of the background. To avoid sudden noise spikes we require that the signal continues to increase for at least 5 successive height intervals. Cloud top is determined in this height where the signal is greater than the calculated standard deviation of the noise above the cloud top. This method was proposed by Platt et al. (1994). Mid-cloud height is defined as the geometric center of cirrus cloud.

3.1 Methods for the retrieval of cirrus optical characteristics

3.1.1 Klett-Fernald method

Most of the methods that have been developed to retrieve the optical properties of cirrus clouds depend on the solution of the standard lidar equation. Generally, the two unknowns of this equation, the backscatter and extinction coefficients, have to be related using either empirical or theoretical methods in order to be able to invert the

lidar equation. There have been many discussions regarding the solutions of the lidar equation and more details can be found in the following articles: Barrett and Ben-Dov, 1967; Viezee et al., 1969; Davis, 1969; Fernald, 1972; Platt, 1973, 1979; Klett, 1981; Fernald, 1984; and Ansmann et al., 1992.

The forward solution of the backscatter coefficient was found to become rapidly unstable for optical depths greater than unity, unless the lidar ratio was specified with extreme accuracy (Platt, 1979). Klett (1981) showed that a backward solution of backscatter coefficient was inherently stable. However, Fernald (1984) further pointed out that stability does not necessarily mean accuracy. The backscatter coefficient and mean lidar ratio can be retrieved, using both Klett and Fernald formalism, as Ansmann et al. (1992) proposed. Once the altitude base and top of the cloud are chosen as a priori, the forward and backward integration can be applied for different values of lidar ratio, until the backscatter coefficients above and below the cirrus cloud become equal to zero. This lidar ratio value, in most of the cases, leads the forward and backward integration to coincide to the desired degree of accuracy (Ansmann et al., 1992). Although the extinction-coefficient profile can be incorrect because of the unrealistic assumption of a range independent lidar ratio, the determined backscatter coefficient profile, the cloud optical depth, and the mean cloud extinction-to-backscatter ratio, can be still obtained with high temporal resolution and acceptable accuracy (Ansmann et al., 1992).

An example of the Klett-Fernald method is presented. At the 20 May, 2006, a cirrus cloud was observed. The base of the cloud was detected at 7700 m while the top of the cloud was at 10 500 m. In Fig. 1 we present backscatter coefficient profiles for three values of (effective) lidar ratio (10, 15 and 20 sr) and we can easily conclude that solutions for the value of 15 sr lead to zero backscatter coefficient above and below the cirrus cloud. At this value we can see that the forward and backward solutions tend to give the same backscatter profile. The effective optical depth can then be calculated to be 0.13.

3.1.2 Transmittance method

In the second method, henceforth called the transmittance method, the optical depth of the cirrus cloud can be determined by comparing the backscattering signals just bellow and above the cloud in the case whence the lidar signals correctly represented the scattering medium (Platt, 1973; Young, 1995; Chen et al., 2002). In order to use this method we apply two linear fits of the scattering signals just below and above the cirrus cloud. The transmission of the cirrus cloud and thus the effective optical depth can then be calculated (Chen et al., 2002). From the calculated backscatter profile, as given by the Klett-Fernald method, we can estimate the effective lidar ratio.

In Fig. 2 we present the range corrected lidar signal for the 20 May 2006. The black line corresponds to the simulated molecular profile which was calculated by the use of an air density profile obtained from a standard atmosphere model (U.S. Standard Atmosphere, 1976) adjusted to the measured ground-level temperature and pressure values. The dashed and dotted lines are the corresponding linear fits of the lidar signal at the cloud base and cloud top respectively. In this case study the transmitance of the cloud is estimated at 0.87 and so the calculated (effective) optical depth is equal to 0.14. This effective optical depth leads to the estimation of effective lidar ratio at 17sr, taking into account the backscatter profile as computed by the Klett-Fernald method.

3.1.3 Raman method

The Raman method is based on the measurement of the elastic-backscatter signal at 355 nm and of the nitrogen inelastic-backscatter signal at 387 nm which permits the determination of the extinction and backscatter coefficients independently of each other and thus, of the extinction-to-backscatter ratio (Ansmann et al., 1992). With the present experimental setup, (355 nm Raman lidar), applications are limited to night time measurements because of the fact that the weak inelastic backscatter signal can only be detected in the absence of the strong daylight background. For the final calculation of extinction coefficient at 355 nm, we calculate the derivative of the algorithm of the

ACPD
7, 9283–9317, 2007

EGU

ratio between the atmospheric number density and the range-corrected lidar-received power. For ice particles, which are usually large compared to the laser wavelength, the wavelength dependence between the extinction at 355 and 387 nm is consider equal to zero (Ansmann et al., 1992).

Figure 3 presents the calculated (effective) extinction (Fig. 3a) and backscatter (Fig. 3b) coefficients and thus the effective lidar ratio profile (Fig. 3c) as computed for 20 May 2006. The integration of the extinction coefficient leads to an effective optical depth of 0.17 while mean effective lidar ratio is calculated to be equal to 26±7 sr.

3.2 Multiple scattering effect

The transmittance of a light beam through a cloud is increased by multiple scattering effects in which photons that have been scattered out of the sampling volume of the lidar in one scattering event may be returned to the lidar field of view in subsequent scattering events. Also, photons that are scattered at shallow forward angles are not lost from the lidar beam and may experience further scattering (Young, 1995). Multiple scattering is significant in cirrus clouds and varies with cloud optical depth, cloud extinction and lidar penetration depth (Wang et al., 2005). As Wandinger (1998) showed, multiple-scattering errors of measured extinction coefficients are typically in the order of 50% at the bases of clouds and decrease with increasing penetration depth to below 20%. Also, Wang et al. (2005) showed that the presence of multiple scattering can lead to an underestimation of the extinction coefficient by as large as 200%, whereas the backscattering coefficient is almost unaffected.

The retrieval of optical properties, as showed previously, leads to effective values of optical depth and lidar ratio. The receiver field of view of the LAP lidar is 1 mrad and thus the effective values are considerably influenced by multiple scattering. The approach to correct the estimated values of cirrus optical depth and lidar ratio depends on the applied method. For transmittance methods we assume a range-independent parameter. Following previous studies (Platt et al., 1987; Sassen and Cho, 1992; Chen et al., 2002), a factor η is introduced, which describes the multiple scattering effect,

ACPD
7, 9283–9317, 2007

henceforth called multiple scattering factor. The smaller η is the more important the multiple scattering effect is. According to Chen et al. (2002) the multiple scattering factor, for a cirrus cloud with an optical depth τ_c , is calculated by Eq. (1).

$$\eta = \frac{\tau_c}{\exp(\tau_c) - 1} \tag{1}$$

For the Raman and Klett-Fernald methods a different approach for dealing with multiple scattering effect is used. The effective extinction coefficient $a_{\text{eff}}(z)$, is related to the actual (single-scattering) coefficient $a(z)$ through a parameter $F(z)$ (here called multiple scattering parameter), as Eq. (2) shows (Wandinger, 1998; Wang, 2002).

$$a_{\text{eff}}(z) = (1 - F(z)) * a(z) \tag{2}$$

We should notice here that the ratio of the effective optical depth to the actual optical depth corresponds to multiple scattering factor, η, and thus to mean value of *(1-F(z))*.

Multiple scattering parameter, $F(z)$ can be estimated through Eq. (3) (Wang et al., 2005), when the ratio of total signal $P_{\text{tot}}(z)$, to single-scattering signal $P_1(z)$ is known.

$$F(z) = \frac{\frac{d}{dz} \ln \frac{P_{\text{tot}}(z)}{P_1(z)}}{2a_{\text{eff}}(z) + \frac{d}{dz} \ln \frac{P_{\text{tot}}(z)}{P_1(z)}} \tag{3}$$

A radiative transfer model, provided by Hogan (2006), has been applied to estimate the relative contribution due to individual orders of multiple scattering. This model has been compared to Eloranta's model (Eloranta, 1998) for a wide range of cloud profiles and lidar parameters and found that reproduces the high-order Eloranta calculation when the latter takes into account 5th or 6th order scattering (Hogan, 2006). This model was also used by Seifert et al. (2007)[1] to estimate the contribution of multiple scattering effects to the effective optical properties of cirrus clouds during Indian Ocean Experiment (INDOEX).

A laser beam of 0.5 mrad full-angle divergence with a wavelength of 355 nm, and a receiver field of view of 1 mrad are used in the model simulation. A problem in this

simulation is the unknown size of the scatterers in the cloud. The used model implies hexagonal ice crystals. To estimate an approximate value of effective radius, which is needed as input for the model, we use the values given by Wang and Sassen (2002), who had related the effective radius with cirrus cloud temperature. The model also requires the single scattering extinction profile and the lidar ratio to estimate the total attenuated backscatter which is the backscatter influenced both by attenuation and multiple scattering effect. The model can also extract six individuals backscatter components (single, double and triple order of scattering for cloud and molecular atmosphere). However, the measurement provides as an output either the effective (total) value of extinction coefficient (Raman method) or the effective value of backscatter coefficient (Klett-Fernald). For this reason, as first input we use the effective value of extinction for the Raman method and the effective backscatter coefficient multiplied by a constant lidar ratio for the Klett-Fernand method. From the computed ratio of the total attenuated backscatter profile to single attenuated backscatter coefficient we can make a first estimation of the multiple scattering parameter F(z), as described in the studies of Wandinger (1998) and Wang et al. (2002). Then, a first estimation of the single-scattering extinction profile can be retrieved. A second or third step is applied in order to estimate the parameter F(z) and thus the correct single scattering extinction profile.

The contribution of multiple scattering effects to the optical properties of the cirrus cloud for the case study of 20 May 2006 and for the Raman method is presented in Fig. 3 (solid lines with circles). The multiple scattering parameter $F(z)$ is decreasing with penetration height, as shown in Fig. 3d. This means that the multiple scattering error of effective extinction coefficients decrease with increasing penetration depth. The profile averaged multiple scattering parameter F, for the Klett-Fernald and Raman methods, are 0.33 and 0.36 respectively. The difference between these parameters is small and is justified by the fact that in the Klett-Fernald method we introduce as input the backscatter coefficient profile multiplied by the corresponding constant lidar ratio, while in the Raman method we input the extinction coefficient profile. For the Klett-

ACPD
7, 9283–9317, 2007

Fernald method the resulting optical depth will be 0.18 and lidar ratio will be 22 sr. For the Raman method these values are 0.25 and 34 sr respectively. However, the multiple scattering factor η, which is calculated for the transmittance method and corresponds to the profile averaged value of $(1 - F(z))$, is equal to 0.93, much greater than the profile averaged model estimated values of $(1 - F(z))$ which are equal to 0.67 and 0.64, for the Klett-Fernald and Raman methods, respectively. Thus, for the transmittance method, multiple scattering effects will introduce a small change to the effective optical depth and lidar ratio, calculated to 0.15 and 18 sr respectively.

4 Results and discussion

During the period 2000–2006, 65 measurements of cirrus clouds were performed, 15 of them were night-time measurements and 50 were day-time measurements. In Fig. 4 a histogram of the number of cirrus occurrence (black) and the total number of measurements as a function of month is presented.

Cirrus clouds are more frequently observed in autumn and spring than in summer whereas. bad weather conditions is the reason for low frequency of lidar measurements during winter-time. For that reason, the frequency occurrence will not be representative, and is not presented here. The maximum probability of observing cirrus cases, as measured by the lidar system, is found to be during spring months, while the minimum probability is found during summer months.

4.1 Geometrical and temperature characteristics

As other studies have shown (Heymsfield and Platt, 1984; Platt and Harshvardhan, 1988; Sassen and Comstock, 2001; Wang and Sassen, 2002), temperature is an important factor in determing cirrus cloud properties because of the strength of the adiabetic process. Platt et al. (1987), Mace et al. (2001), and Sassen and Comstock (2001) have also shown that cloud thickness is another significant factor that influences cirrus

properties. Thus, using our database, we examine and present (Table 1) yearly and seasonal means and variability in several geometrical and temperature characteristics of cirrus clouds, as they calculated at the mid-latitude station in Thessaloniki during the period 2000–2006.

All temperatures are obtained from radiosondes, launched at Thessaloniki airport, twice per day, at 00:00 UTC and 12:00 UTC. Mid-cloud temperature is defined as the temperature that corresponds to mid-cloud height. The boundaries of the cloud were determined as presented in the methodology section.

Cirrus clouds are generally observed in the mid-altitude region from 7 to 12 km, with mid-cloud temperatures ranging from –65° to –25°C. The cloud thickness is generally in the range from 0.85 to 5 km, with 37% of our cases have thickness between 2 and 3 km. As can be seen from Table 1, the lowest cirrus clouds are observed in winter. This has been also found in the study of Sassen and Campell (2001). Platt et al. (1987), had studied mid-latitude cirrus clouds and found that winter cirrus clouds base lies at 7.38km, while for summer cirrus clouds base found a larger value of 7.79 km. These values are in general agreement with our results.

Cirrus cloud properties follow seasonal cycles and this is demonstrated especially in the temperature's values. In winter and autumn, the top of cirrus clouds is observed just below the tropopause, meanwhile in spring it is observed just above the tropopause. However, during summer, the mean tropopause height over Thessaloniki is of the order of 12.9 km, while the mean cirrus top height is somewhat below the tropopause (around 11.2 km). Not unexpectedly, cirrus frequency is the lowest of the year in summer, as one can see in Fig. 4.

A scatter plot of mid-cloud temperature with mid-cloud height for all of our cases is shown in Fig. 5. The cloud temperature decreases with increase of the cloud altitude as expected. Averaged values of mid cloud temperatures grouped at 10°C intervals are also shown in Fig. 5 as full circles.

Figure 6 shows the location of the cloud base and top heights in relation to the tropopause height. Here we use the convectional tropopause height as defined by

WMO (World Meteorological Organization). This is defined as the lower boundary of an atmospheric layer in the upper troposphere in which the temperature lapse rate is less than 2°C km^{-1} and this layer has to be at least 2 km thick (Krishna Murthy et al., 1986). A 30-day moving average was applied to the tropopause height time series. The height of tropopause exhibits a seasonal variability with values ranging between ~10 km in the winter and ~15 km in the summer. Cirrus cloud tops are observed near the tropopause, while all cloud bases are within the troposphere. From our data analysis, 44% of the cirrus cases found had cloud top heights ±0.5 km from the tropopause heights as derived by the radiosonde data. Only 5% of cirrus cases shows cloud top height higher than the above altitudes.

4.2 Optical properties of cirrus clouds

We have applied the methods which were briefly presented in the methodology section to the measured lidar data. From 65 of our cases the Klett-Fernald method gave a reliable result to 53 of said cases, while the transmittance method gave a reliable result to 40 of them. The reasons why these methods do not give reliable results in certain cases are discussed later. Figure 7 shows the direct comparison of the optical depth at 355nm as derived from the three methods, after taking into account multiple scattering effects. The two sets of independently derived optical depth are in good agreement, with a correlation coefficient of 0.74 for the Transmittance/Klett-Fernald comparison and of 0.92 for the Raman/Klett-Fernald comparison.

For 14 common cases using the analyses based on the Klett-Fernald, transmittance and Raman methods the mean optical depths were calculated to be 0.41±0.27, 0.39±0.25 and 0.38±0.28, while the lidar ratio values were found at 28.5±17.3, 26.9±14.8 and 30.8±17.8 sr respectively. For 34 common cases of Klett-Fernald and transmittance methods, the mean optical depths values were 0.36±0.26 and 0.35±0.26, while the lidar ratio values were 31.9±16.2 and 28.8±23.4 sr respectively. The calculated values for both optical depth and lidar ratio are generally in good agreement taking into account that the transmittance method uses only the elastic signal

while Klett-Fernald formalism use the assumption of a range independent lidar ratio for solving the single scattering lidar equation and in addition the fact that the Raman method uses both elastic and inelastic backscatter signals.

The reason that Klett-Fernald method cannot give a reliable result in all of our cases is the numerical instability inherited when optical depths are very low. In cases when the cirrus cloud is optically thin, this method is not effectively affected by changes to the lidar ratio values and so no lidar ratio can be representative. The disagreement between the Klett-Fernald and Raman methods exists in some cases because of the assumption of a vertically constant lidar ratio for the solution of elastic differential equation. In these cases we have found that lidar ratios derived from the Klett-Fernald method tend to agree with the lidar ratio of the lowest layer of the cirrus cloud. The backscatter coefficients as were calculated with the Klett-Fernald and Raman methods showed the same results for the measured aerosol layers. This means that the two methods give reliable profiles of backscatter coefficients. In the transmittance method, as we have already mentioned, the divergence of the signal between the bottom and top of the cloud can procure the real transmittance of the cloud and thus the optical depth. In these cases, we should notice that various initial conditions can influence the assumption of purely molecular backscatter signal at the cloud base. Moreover, when the signal is too noisy at the top of the cloud, or there are some lower layers that cannot be distinguished, the applying fit can lead to erroneous values of optical depth and lidar ratio.

Figure 8a shows the monthly mean values of cirrus optical depths while 8b the percentage occurrence of cirrus measurements as a function of optical depth, as were calculated from the Klett-Fernald method, for each seasons. The most prevalent region of cirrus optical depth values is between 0.1 and 0.2. We have found that 7.5% of cirrus clouds are sub-visual (optical depth <0.03), 51% of cirrus clouds are optically thin (optical depth between 0.03 and 0.3) and 41.5% of cirrus clouds are opaque (optical depth >0.3). Sassen and Campbell (2001) had found that cirrus clouds optical depths were below 0.3 for 50% of the cases included into their mid-latitude station

ACPD
7, 9283–9317, 2007

EGU

cirrus climatology analysis.

In Table 2, we present the mean values of optical depth and lidar ratio as were calculated for all of our cases, before and after correction for multiple scattering effects. The values which are presented in table 2 are not directly comparable, as they are not referring to the same cases of cirrus clouds. We should notice that the mean optical depth as derived from the transmittance method is quite high because of the problems of the determination of low optical depths, as discussed previously.

The values in Table 2 may be compared with other climatological studies. Sassen and Comstock (2001) had studied mid-latitude cirrus clouds, using an extended database, and found mean optical depths of 0.75±0.91 at 694 nm, while lidar ratio was calculated at 24 sr. Wang and Sassen (2002), had also studied mid-latitude cirrus clouds, for the period 1996–2000, and found that most cirrus clouds were optically thin with a mean effective optical depth of 0.58±0.67. Cirrus climatological results from Observatoire de haute Provence in France are presented by Goldfarb et al. (2001) and suggest as more prevalent optical depth in the region from 0.03 to 0.1. In addition, Seifert et al. (2007)[1] have studied the optical properties of cirrus clouds over the tropical Indian ocean during Northeast (NE) and Southwest (SW) monsoon seasons. They found a multiple-scattering corrected optical depth of 0.25±0.26 (NE) and 0.34±0.29 (SW), while lidar ratio values were found to be 33±9 sr (NE) and 29±11 sr (SW).

We can further compare the contribution of multiple scattering effects as calculated for the different methods. The range-independent parameter η that is used in the transmittance method has a mean value of 0.86±0.02. However, the corresponding profile averaged parameter $(1 - F(z))$, which is used in Klett-Fernald and Raman methods, is smaller and mostly ranges from 0.6 to 0.75. This means that the contribution of multiple scattering effects as applied in the transmittance method is smaller than the calculated contribution to the Klett-Fernald and Raman methods, especially when we are referring to optical thin cirrus clouds. We have also found that the multiple scattering parameter $F(z)$ is decreasing with penetration height. This means that multiple scattering errors of measured extinction coefficients decrease with increasing penetration depth. Similar

ACPD
7, 9283–9317, 2007

results were reported in Wandinger (1998). Assuming that backscatter coefficient is almost unaffected from multiple scattering, lidar ratio errors are affected only by the extinction-coefficient errors.

4.3 Temperature and thickness dependencies on cirrus optical properties

The dependence of cirrus cloud thickness on mid-cloud temperature is presented in Fig. 9. Thicker clouds (~3 km) are observed at temperatures of ~–45°C, decreasing in thickness both for higher and lower temperatures. Platt et al. (1987), showed a well defined peak at higher temperatures around –40°C for mid-latitude clouds. Our results are in agreement with Sassen and Comstock (2001) who have also presented the dependence of cloud thickness on mid-cloud temperature. Sunilkumar and Parameswaran (2005) studied tropical cirrus clouds and found that this peak is shifted to lower temperatures, in the range of –50° to –70°C. The conclusion of Sunilkumar and Parameswaran (2005) that mid-latitude cirrus clouds are generally warmer and thicker than those over the tropics is in agreement with our results. However, we should keep in mind that the number of samples corresponding to temperatures below –60°C is limited.

The dependence of optical depth on cirrus thickness is shown in Fig. 10a and on mid-cloud temperature in Fig. 10b. There is an indication that optical depth increases with increasing thickness. Sassen and Comstock (2001) showed that these parameters follow a linear relation.

As we have mentioned before, cirrus cases analysis that refer to temperatures of lower than –60°C are of low significance. For the remaining data shown in Fig. 10b there are indications that the cloud optical depth increases as the mid-cloud temperature increases. We should keep in mind that increasing thickness of cirrus clouds also tends to increase the mid-cloud temperature. Other studies have also investigated the dependence of optical depth on mid-cloud temperature and found that these parameters are connected either linearly (Sassen and Comstock, 2001) or through a second-order polynomial function (Sunilkumar and Parameswaran, 2005; Platt et al., 1987). Our results, as shown in Figs. 9 and 10, are indicative only and more cases

ACPD
7, 9283–9317, 2007

should be collected to our database for a more accurate conclusion. We have also studied the dependence of lidar ratio on thickness and mid-cloud temperature and no clear tendency was found.

5 Summary and conclusions

This study provides an analysis of the geometrical and temperature characteristics as well as the optical properties of mid-latitude cirrus clouds. Our results show that cirrus clouds were observed between 7 to 12 km, with mid-cloud temperatures ranging from –65° to –25°C and a mean thickness of 2.8 km. Cirrus clouds top heights typically approach the tropopause, except for the summer months. 44% of cirrus clouds top heights are observed 0.5 km above or below the tropopause. The seasonality of cirrus clouds properties was also investigated with minimum frequency of occurrence of cirrus clouds in the summertime, when the mean temperature of the cloud top is the highest of the year.

We have also provided the optical properties of mid-latitude cirrus clouds as were calculated through three different methods. A mean optical depth of 0.3±0.24 and a mean lidar ratio of 28±17 sr were found with the use of the Klett-Fernald formalism. Sub-visual cirrus clouds represent 13% of our measurements before the correction for multiple scattering while this percentage is reduced to 7.5%, after the correction. In addition, we have compared the resulting optical depth and lidar ratio and found a good agreement between the three methods used. The comparison has been performed to the single-scattering values of the optical depths and correlation coefficients of 0.74 and 0.92 were found for the Transmittance/Klett-Fernlad method and the Raman/Klett-Fernlad method respectively. In the following we report briefly the benefits and restrictions of each method.

The main advantage of the Transmittance method is that it does not require any microphysical hypotheses about cirrus clouds. However, this method depends on the condition of the atmosphere outside the cloud because the presence of aerosol parti-

ACPD
7, 9283–9317, 2007

cles can affect the lidar signals significantly due to Rayleigh scattering effects. Another limitation of this method is that optically thin cirrus clouds have too low optical depth to produce rapid enough convergence for the solution. In that case there are more uncertainties related with the errors in the estimation of the boundary height or for noise or offset calculations of the lidar signal at the calibration range, as also Young (1995) have presented. On the other hand, the Klett-Fernald method uses a strong elastic-backscatter signal that is several orders of magnitude larger than the Raman signal in order to retrieve the backscatter coefficient. This is considered as a main benefit of this method. However, to solve the lidar equation through the Klett-Fernald formalism we assume a range independent lidar ratio. The accurate estimation of the extinction coefficient is possible through the Raman lidar technique and thus makes this method a powerful tool for cirrus studies. The independent measurement of backscatter and extinction profiles and thus lidar ratio profiles is only possible through the Raman method. Nevertheless, this method can be applied only for night- time measurements.

We have also investigated the dependence of optical properties on temperature and geometrical characteristics. A maximum mid-cloud depth is in the range of 3 to 4 km at temperatures between –50°C and –45°C, and decreases both for lower and larger temperatures. An indication that optical depth increases with increasing thickness and mid-cloud temperature is found, while a more extended database is needed to strengthen this indication. We have also examined the dependence of lidar ratio on both thickness and mid-temperature and no clear tendency was found. Our results seem to demonstrate that mid-latitude cirrus clouds are warmer, lower and thicker than tropical cirrus clouds.

Acknowledgements. The financial support of this work by the Hellenic Ministry of Development – Greek Secretariat for Research and Technology (PENED) is greatly acknowledged. Measurements were performed in the frame of the EU-funded EARLINET and EARLINET-ASOS projects (EVR1-CT1999-40003 and RICA 025991). Radiosonde data for Thessaloniki were kindly provided by the Hellenic National Meteorological Service.

References

Amiridis, V., Balis, D. S., Kazadzis, S., Bais, A., Giannakaki, E., Papayannis A., and Zerefos, C: Four-year aerosol observation with a Raman lidar at Thessaloniki, Greece, in the framework of EARLINET, J. Geophys. Res., 110, D21203, doi:10.1029/2005JD006190, 2005.

Ansmann, A., Wandinger, U., Riebesell, M., Weitkamp, C., and Michaelis, W.: Independent measurement of extinction and backscatter profiles in cirrus clouds by using a combined Raman elastic backscatter lidar, Appl. Opt., 31, 7113–7131, 1992.

Balis D. S., Amiridis, V., Zerefos., C., Gerasopoulos, E., Andreae, M., Zanis, P., Kazantzidis, A., Kazadzis, S., and Papayannis, A.: Raman lidar and sunphotometric measurements of aerosol optical properties over Thessaloniki, Greece during a biomass burning episode, Atmos. Environ., 37, 4529–4538, 2003.

Barrett, E. W. and Ben-Dov, O.: Application of the lidar to air pollution measurements, J. Appl. Meteorol., 6, 500–515, 1967.

Cadet, B., Goldfarb, L., Faduilhe, D., Baldy, D., Giraud, V., Keckhut, P., and Rechou, A.: A subtropical cirrus clouds climatology from Reunion island (21° S, 55° E) lidar data set, Geophys. Res. Lett., 30(3), 1130, doi:10.1029/2002GL016342, 2003.

Chen W. N., Chiang, C. W., and Nee, J. B.: Lidar ratio and depolarization ratio for cirrus clouds, Appl. Opt., 41, 6470–6476, 2002.

Comstock, J. M. and Ackerman, T.: Ground-based lidar and radar remote sensing of tropical cirrus clouds at Nauru island: Cloud statistics and radiative impacts, J. Geophys. Res., 107(23), 4714, doi:10.1029/2002JD002203, 2002.

Davis, P. A.: The analysis of lidar signatures of cirrus clouds, Appl. Opt., 8, 2099–2102, 1969.

Eleftheratos K., Zerefos, C., Zanis, P., Balis, D. S., Tselioudis, G., Gierens, K., and Sausen, R.: A twenty-year study on natural and manmade global interannual fluctuations of cirrus cloud cover, Atmos. Chem. Phys., 7, 93–126, 2007, http://www.atmos-chem-phys.net/7/93/2007/.

Eloranta, E.: Practical model for the calculation of multiply scatterd LIDAR returns, Appl. Opt., 37, 2464–2472, 1998.

Fahey, D. W. and Schumann, U.: Aviation-Produced Aerosols and Cloudiness, Chapters 3 in Aviation and Global Atmosphere, A Special Report of IPCC (Intergovernmental Panel on Climate Change), J. E. Penner, D. H. Griggs, D. J. Dokken, M. McFarland, Cambridge University Press, Cambridge, UK, 65–120, 1999.

Fernald, F. G., Herman, B. M., and Reagon, J. A.: Determination of aerosol height distributions by lidar, J. Appl. Meteorol., 11, 482–489, 1972.
Fernald, F. G.: Analysis of atmospheric lidar observations; some comments, Appl. Opt., 23, 652–653, 1984.
Fu, Q., and Liou, K. N.: Parameterization of the Radiative Properties of Cirrus Clouds, J. Atmos. Sci., 50, 2008-2025, 1993.
Goldfarb L., Keckhut, P., Chanin, M.-L., and Hauchecorne, A.: Cirrus climatological results from lidar measurements at OHP (44° N, 6° E), Geophys. Res. Lett., 28, 1967–1690, 2001.
Heymsfield, A. J. and Platt, C. M. R.: A parameterization of the particle size spectrum of ice clouds in terms of the ambient temperature and the ice water content, J. Atmos. Sci., 41, 84-6-855, 1984.
Hogan, R.: Fast approximate calculation of multiply scattered lidar returns, Appl. Opt., 45, 5984–5992, 2006.
Klett, J. D.: Stable analytical inversion solution for processing lidar returns, Appl. Opt., 20, 211–220, 1981.
Krishna Murthy, B. V., Parameswaran, K., and Rose, K. O.: Temporal variations of the tropical tropopause characteristics, J. Atmos. Sci., 43, 914–922, 1986.
Mace, G. G., Clothiaux, E. E., and Ackerman, T. P.: The composite characteristics of cirrus clouds: Bulk properties revealed by one year continues cloud radar data, J. Climate, 14, 2185–2203, 2001.
Matthias, V., Bosenberg, J., Freudenthaler, V., Amodeo, A., Balin, I., and Balis, D.: Aerosol lidar intercomparison in the framework of EARLINET project: 1. Instruments, Appl. Opt., 43, 961–976, 2004
Platt, C. M. R.: Lidar and radiometric observations of cirrus clouds, J. Atmos. Sci., 30, 1191–1204, 1973.
Platt, C. M. R.: Remote sounding of high clouds. I: Of visible and infrared optical properties from lidar and radiometer measurements, J. Appl. Meteorol., 18, 1130–1143, 1979.
Platt, C. M. R., Scott, J. C., and Dilley, C.: Remote sounding of high clouds. Part VI: Optical properties, J. Atmos. Sci., 44, 729–747, 1987.
Platt, C. M. R. and Harshvardhan: Temperature dependencies of cirrus extinction: implications for climate feedback, J. Geophys. Res., 93, 11 051-11 058, 1988.
Platt, C. M. R., Young, S. A., Carswell, A. I., Pal, S. R., McCormick, M. P., Winker, D. M., DelGuasta, M., Stefanutti, L., Eberhard, W. L., Hardesty, M., Flamant, P. H., Valentin, R.,

Forgan, B., Gimmestad, G. G., Jager, H., Khmelevtsov, S., Kovel, I., Kaprieolev, B., Lu, Da-ren, Sassen, K., Shamanaev, V. S., Uchino, O., Mizuno, Y., Wandinger, U., Weitkamp, C., Ansmann, A., and Wooldridge, C.: The experimental cloud lidar pilot study (ECLIPS) for cloud-radiation research, Bull. Am. Meteorol. Soc., 75, 1635–1654, 1994.

Sassen, K. and Cho, B.Y.: Subvisual-thin cirrus lidar dataset for satellite verification and climatological research, J. Appl. Meterorol., 31, 1275–1285, 1992.

Sassen, K. and Campbell, J. R.: A midlatitude cirrus cloud climatology from the facility for atmospheric remote sensing, part I: Macrophysical and synoptic properties, J. Atmos. Sci., 58, 481–496, 2001.

Sassen K. and Comstock, J.: A midlatitude cirrus cloud climatology from the facility for atmospheric remote sensing. Part III: Radiative properties, J. Atmos. Sci., 58, 2113–2127, 2001.

Stephens, G. L. and Webster, P.J.: Clouds and Climate: Sensitivity of Simple Systems, J. Atmos. Sci., 38, 235–247, 1981.

Sunilkumar, S. V. and Parameswaran, K.: Temperature dependence of tropical cirrus properties and radiative effects, J. Geophys. Res., 110, D13205, doi:10.1029/2004JD005426, 2005.

Viezee, W., Uthe, E. E., and Collis, R. T. H.: Lidar observations of airfield approach conditions, J. Appl. Meteorol., 8, 274–283, 1969.

Wandinger, U.: Multiple-scattering influence on extinction-and backscatter-coefficient measurements with Raman and high-spectral-resolution lidars, Appl. Opt., 37, 417–427, 1998.

Wang, P., Minnis, P., McCormick, M. P., Kent, G. S., and Skeens, K. M.: A 6-year climatology of cloud occurrences frequency from Stratospheric Aerosol and Gas Experiment II observations (1985–1990), J. Geophys. Res., 101, 29 407–29 429, 1996.

Wang, P., Minnis, P., McCormick, M. P., Kent, G. S., Yue, G. K., Young, D. F., and Skeens, K. M.: A study of the vertical structure of tropical (20° S–20° N) optically thin clouds from SAGE II observations, Atmos. Res., 47–48, 599–614, 1998.

Wang, Z. and Sassen, K.: Cirrus cloud microphysical property retrieval using lidar and radar measurements. Part II: Midlatitude cirrus microphysical and radiative properties, J. Atmos. Sci., 59, 2291–2302, 2002.

Wang X., Boselli, A., Avino, L. D., Velotta, R., Spinelli, N., Bruscaglioni, P., Ismaelli, A., and Zaccanti, G.: An algorithm to determine cirrus properties from analysis of multiple-scattering influence on lidar signals, Appl. Phys. B, 80, 609–615, 2005.

Young S.: Analysis of lidar backscatter profiles in optically thin cirrus, Appl. Opt., 34, 7019–7031, 1995.

Zerefos C. S., Eleftheratos, K., Balis, D. S., Zanis, P., Tselioudis, G., and Meleti, C.: Evidence of impact of aviation on cirrus cloud formation, Atmos. Chem. Phys., 3, 1633–1644, 2003, http://www.atmos-chem-phys.net/3/1633/2003/.

Table 1. Seasonal and yearly averages of various cirrus cloud properties.

Cirrus Properties	WINTER	SPRING	SUMMER	AUTUMN	ANNUAL
Base height (km)	7.25±0.5	8.21± 1.5	8.60 ±1.6	8.98 ± 1.2	8.58 ±1.4
Mid height (km)	8.66±0.8	9.71±1.2	9.94±0.9	10.21±1.2	9.92±1.2
Top height (km)	10.08±1.4	11.27±1.2	11.19±1.3	11.43±1.3	11.27±1.3
Thickness (km)	2.83±1.2	3.06±1.1	2.59±0.8	2.44±0.7	2.68±0.9
Tropopause (km)	10.5±1.3	10.9±1.1	12.9±2.2	12.1±1.23	11.6±1.8
Base temperature (°C)	–34.2±6.4	–37.0±10.4	–32.1±14	–39.4±9.1	–37.5±10
Mid temperature (°C)	–45.5±5.9	–48.9±8.0	–41.7±9.9	–48.8±9.3	–47.8±8.9
Top temperature (°C)	–55.5±9.4	–59.0±7.7	–52.9±9.3	–56.6±9.2	–56.8±8.7

Table 2. Mean optical properties of cirrus clouds for each method before and after correction for multiple scattering.

Method	N° of cases	Effective Optical Depth	Optical Depth	Effective Lidar ratio (sr)	Lidar ratio (sr)
Klett-Fernald	53	0.19±0.18	0.30±0.24	18±11	28±17
Transmittance	40	0.34±0.35	0.49±0.89	25±20	29±23
Raman	15	0.23±0.18	0.35±0.26	24±13	33±20

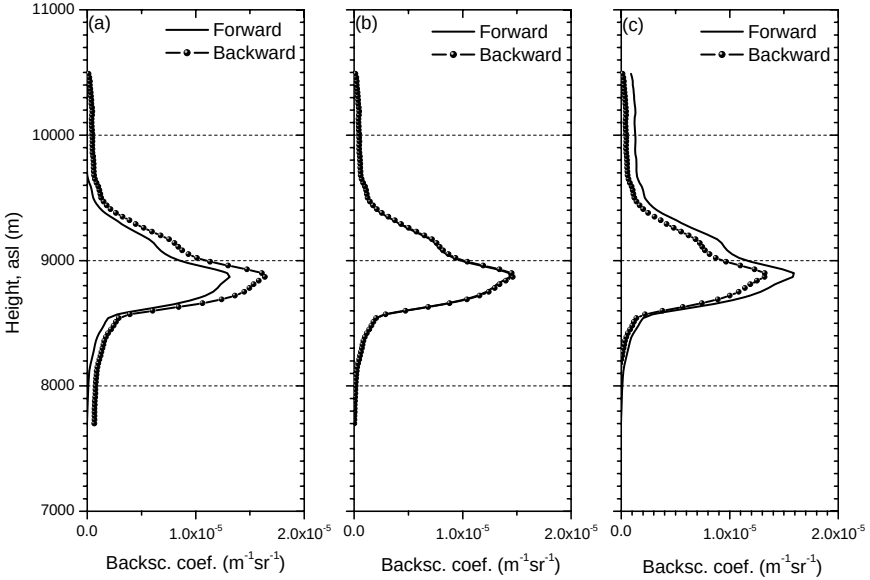

Fig. 1. Forward and backward solutions of lidar equation by assuming a range independent lidar ratio **(a)** lidar ratio = 10 sr, **(b)** lidar ratio = 15 sr and **(c)** lidar ratio = 20 sr.

ACPD
7, 9283–9317, 2007

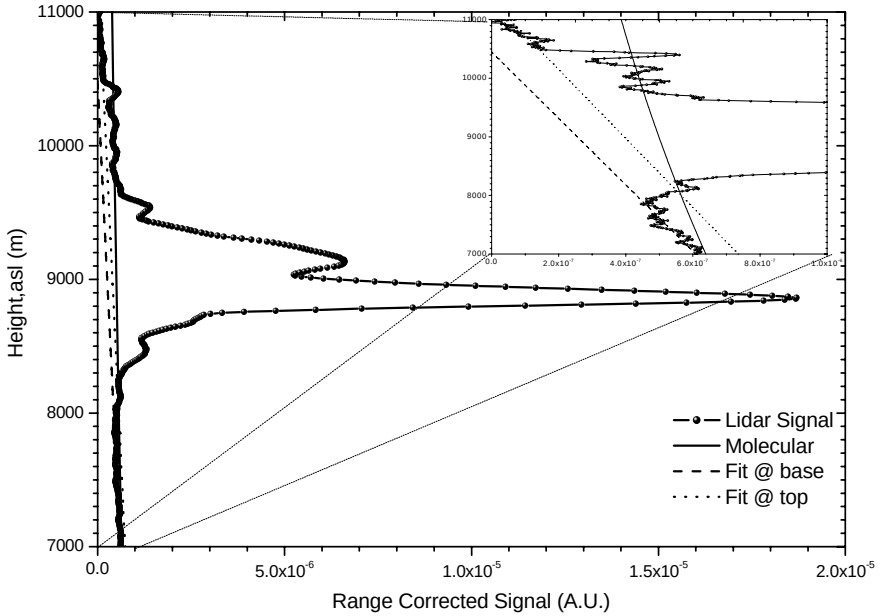

Fig. 2. Range corrected signal, along with molecular atmosphere and the applied fits outside of the cloud region.

ACPD
7, 9283–9317, 2007

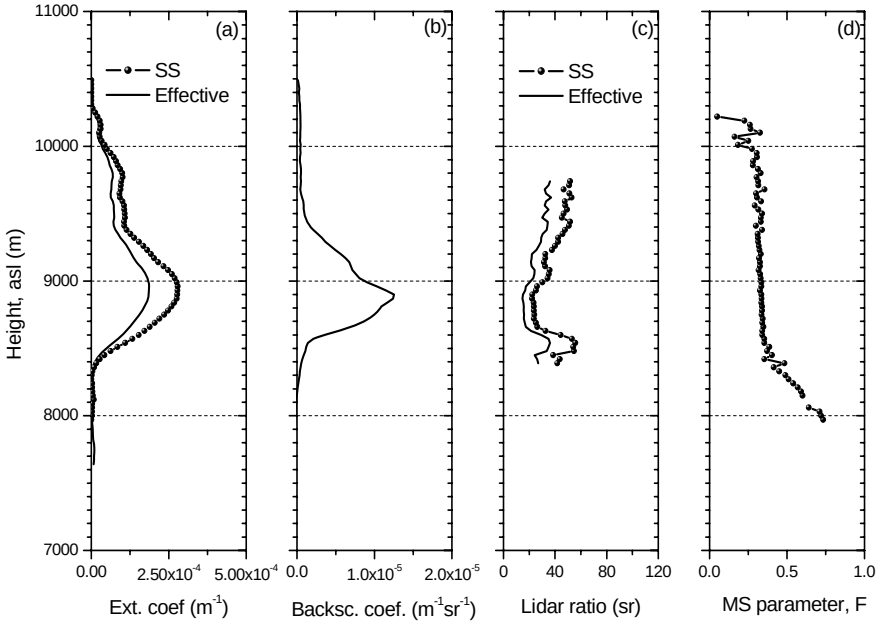

Fig. 3. Profiles of **(a)** extinction coefficient, **(b)** backscatter coefficient, **(c)** lidar ratio before and after the correction for multiple scattering effect and **(d)** multiple scattering parameterpresented climatology for sub-tropical.

ACPD
7, 9283–9317, 2007

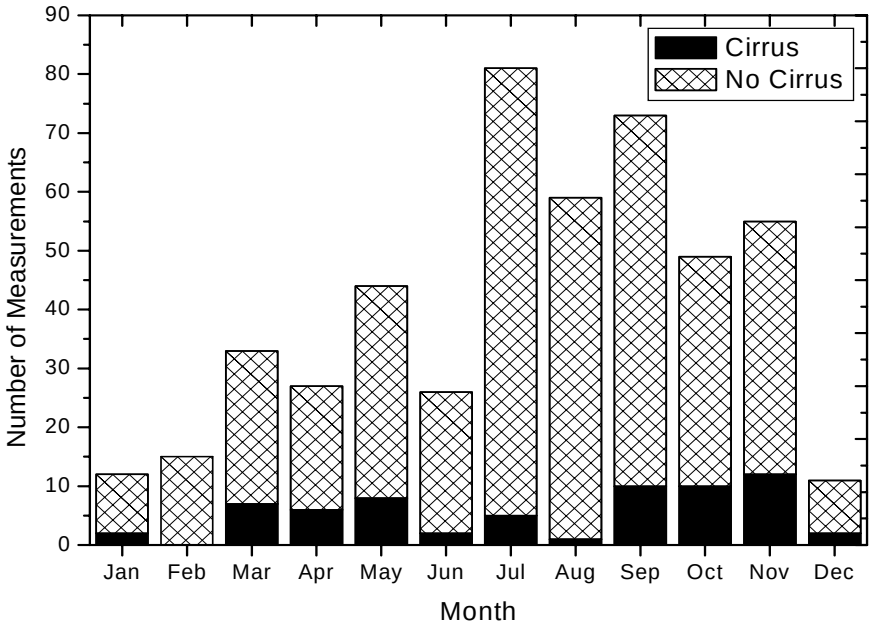

Fig. 4. Histogram of the number of cirrus occurrences and the total number of lidar measurements from 2000 to 2006 as a function of month.

ACPD
7, 9283–9317, 2007

EGU

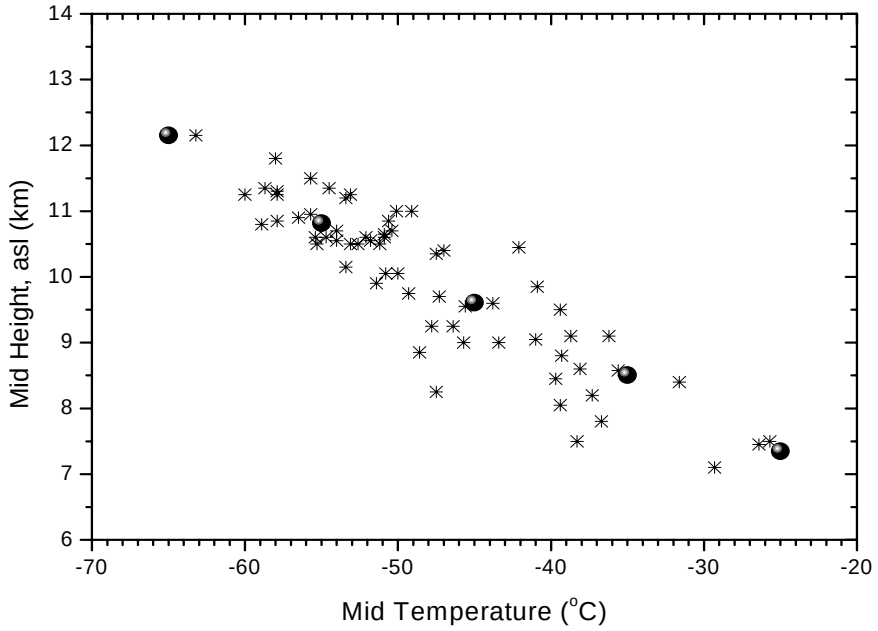

Fig. 5. Scatter plot of mid height with mid temperature. Filled circles present average values grouped at 10°C interval.

ACPD
7, 9283–9317, 2007

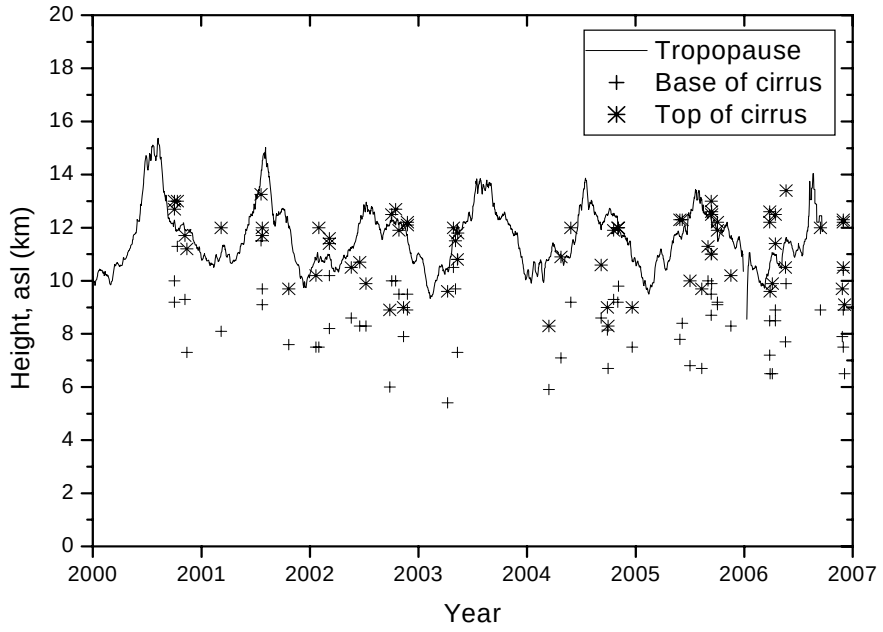

Fig. 6. Timeseries of tropopause height along with cirrus cloud top and cirrus cloud base height.

ACPD
7, 9283–9317, 2007

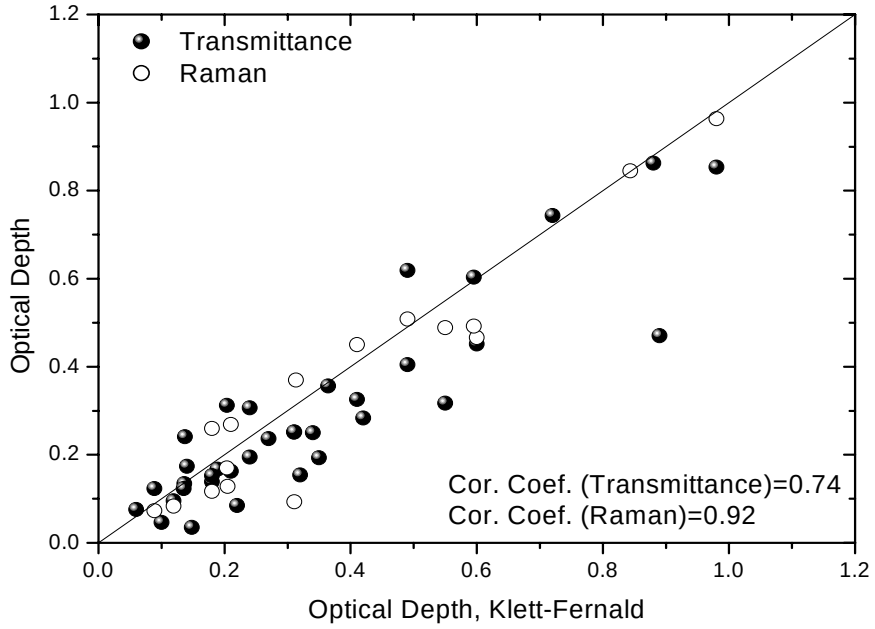

Fig. 7. Comparison of cirrus optical depth of Klett-Fernald method with Transmitance and Raman methods.

ACPD
7, 9283–9317, 2007

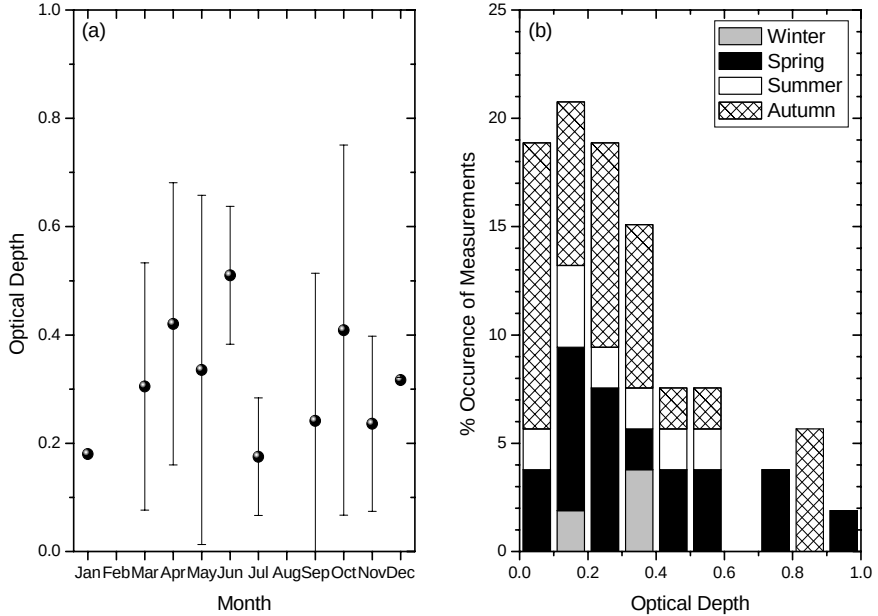

Fig. 8. (a) Monthly variation of optical depth and **(b)** Histogram of cirrus seasonal optical depth.

ACPD
7, 9283–9317, 2007

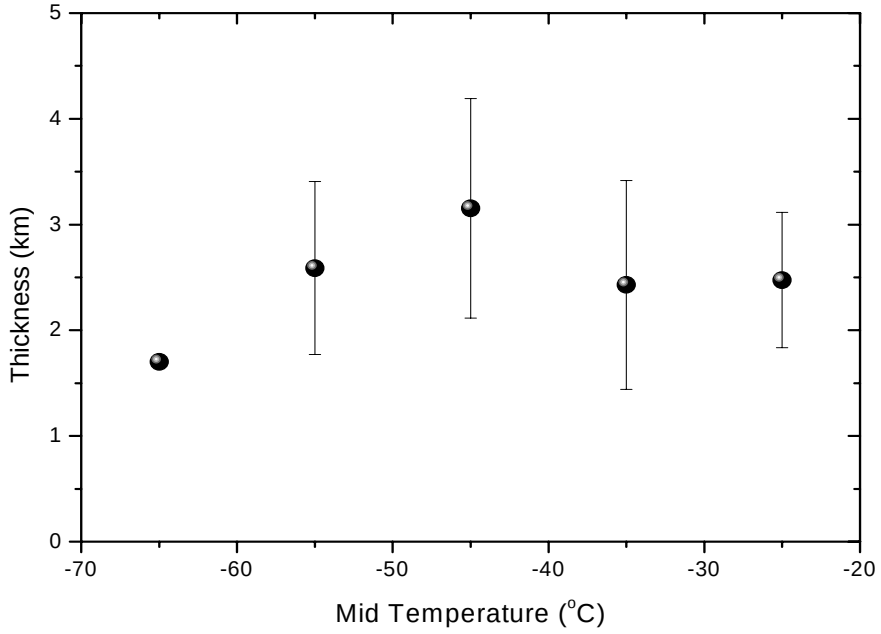

Fig. 9. Dependence of thickness of cirrus cloud on 10°C intervals of mid-cloud temperature.

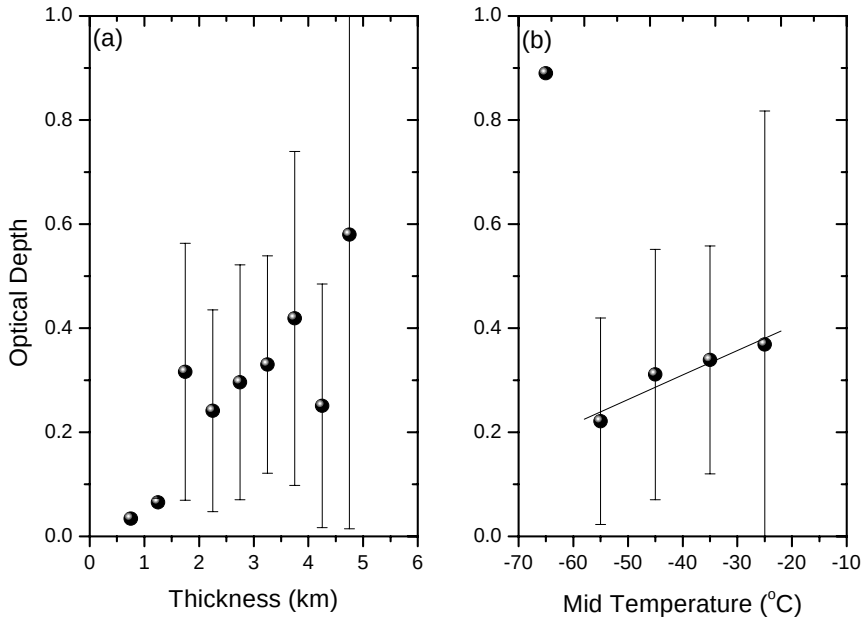

Fig. 10. Depedencies of optical depth on **(a)** 0.5 km intervals of thickness and **(b)** 10°C intervals of mid-cloud temperature.

ACPD
7, 9283–9317, 2007